e-ISSN: 2455-667X

Annals of Natural Sciences
(Peer-Reviewed/Referred International Journal)
Vol. 5(1), March 2019: 55-60
Journal's URL: http://www.crsdindia.com/ans.html
Email: crsdindia@gmail.com

Annals of Natural Sciences

ORIGINAL ARTICLE

Appearance of Dip in Proton-Proton Elastic Scattering Cross-section

J.P. Gupta
Department of Physics, D.S. College Aligarh (UP) India
Email: jpgupta9412328924@rediffmail.com

ABSTRACT

In the case of proton-proton interactions, the variation of differential elastic scattering cross-section as a function of four momentum transfer 't' shows diffraction behavior and a markable dip in the differential cross-section is found near the four momentum transfer t $\approx$ *1.4 (GeV/c)*^{2}*. In the present work an attempt has been made to study the position of the diffraction minima (*t_{dip}*), the position of the secondary maxima (*t_{max}*), the differential scattering cross-sections at the dip and at the secondary maxima. The parameterization of these physical quantities have been proposed for the calculations and the results are compared with the experimental data. The energy dependence of these quantities have also been taken in to account. The proton-proton elastic scattering have been considered for a wide range of centre of mass energy (*$\sqrt{s}$*), from 5.0 GeV. to 2000 GeV.*

Key words: *p-p scattering, h-h scattering, particle-particle interaction, scattering cross-section*

Received: 8th January 2019, Revised: 9th February 2019, Accepted: 17th February 2019

How to cite this article:
Gupta J.P. (2019): Appearance of Dip in Proton-Proton Elastic Scattering Cross-section. Annals of Natural Sciences, Vol. 5[1]: March, 2019: 55-60.

INTRODUCTION

Elastic scattering is the simplest form of interaction between two particles. In elastic scattering process, the angular distribution of the scattering cross-sections have attracted the attention of many workers (Alsad, Z. *et al*., 1983, Abazob, V,M. *et al*., 2012 etc). In the case of proton-proton interactions, the variation of differential elastic scattering cross-section as a function of four momentum transfer 't' shows diffraction behavior and deserves special mention. A markable Dip in the differential cross-section is found near t $\approx$ 1.4 (GeV/c)^2.

The differential elastic scattering cross-section involves, the Coulomb, interference and nuclear amplitudes. In very forward direction the differential cross-section is dominated by the real coulomb amplitude (Castaldi, R. 1985). The magnitude of Coulomb and nuclear amplitudes are of the same order and may give rise to a non-negligible interference effect. The main feature of proton-proton elastic scattering is the appearance of a sharp minima (dip), followed by a secondary maxima (Alsad, Z. *et al*., 1983). Several authors and collaborations (Avila, C. *et al*., 2002, Amos, N.A. 1990 etc) have made detailed studies of the dip structure and its energy dependence. The dip becomes more and more pronounced with increasing energy and then recedes.

In the present work an attempt has been made to study the position of the diffraction minima (t_{dip}), the position of the secondary maxima (t_{max}), the differential scattering cross-sections at the dip and at the secondary maxima. The parameterization of these physical quantities has been proposed for the calculations and the results are compared with the experimental data. The energy dependence of these quantities have also been taken in to

account. The proton-proton elastic scattering have been considered for a wide range of centre of mass energy ($\sqrt{s}$), from 5.0 GeV to 2000 GeV.

THE REGION OF COULOMB–NUCLEAR INTERFERENCE

The most striking feature of high energy proton-proton elastic scattering is the division of the angular distribution of the scattering cross-section into three distinct regions of momentum transfer. The Coulomb-nuclear interference region takes place in the $0.001 \leq |t| \leq 0.01$ $(GeV/c)^2$ region. The Coulomb-nuclear interference effect becomes more and more important as the incident energy increases. Different authors (Negy, E. *et al*., Gauron, P. 1988 etc) fitted the p-p differential scattering cross-section, using the parameterization,

$$d\sigma/dt = \pi [f_c + f_n]^2 \quad .....(1)$$

Where, f_c and f_n are the Coulomb and Nuclear amplitudes respectively.

The relative importance of the interference term is minimum, when the nuclear and Coulomb amplitudes are comparable. The measurement of the interference term allows the determination of the phase of the nuclear scattering amplitude in the forward direction (Castaldi, R. 1985), which is usually expressed as the ratio (ρ) of the real to imaginary part of the scattering amplitudes at four momentum transfer (t)=0.

The real part of the elastic amplitude is related to the imaginary part via dispersion relation (Bronzan, J.B. *et al*., 1974). On the other hand the imaginary part at t = 0, it is related to the total cross-section by the optical theorem. As a consequence, it is possible to write the parameter (ρ) at a given energy as an integral of the total cross-section over energy. Such an integral relation can be approximated by a local expression, which relates (ρ) to the derivative of σ_{tot} with respect to energy,

$$(\rho) = (\pi / 2\, \sigma_{tot})\ d\sigma_{tot}/d \ln s \quad .....(2)$$

THE DIFFRACTION PEAK REGION ($|t| \leq 1.0$ $(GeV/c)^2$

This region of the angular distribution is weakly energy dependent. There is a sharp forward peak for $0.01 \leq |t| \leq 1.0$ $(GeV/c)^2$. The forward peak is generally, recognized to be diffractive or shadow scattering phenomenon (Break-stone, A. *et al*., 1984), caused by the absorptive process in high energy p-p interactions. The data on p-p elastic scattering cross-section is represented by an exponential dependence on 't' (Giacomelli, G. 1979), i.e.,

$$d\sigma/dt = a \exp.(bt) \quad .....(3)$$

Where 'a' and 'b' are two adjustable parameters.

The energy dependence of the slope of the elastic differential cross-section for proton-proton interactions, indicates a shrinkage in the diffraction peak at a rate of at least ln s. The essential energy dependence of shrinking of the diffraction peak is characterized by the increase of 'b' with energy.

LARGE t-REGION

For the four momentum transfer $|t| \leq 1.0$ $(GeV/c)^2$, the angular distribution becomes more and more flat and have a very strong energy dependent (Alsad, Z. *et al.*, 1983). The main feature of the p-p elastic differential cross-section in the large t-region, is a progressive development of a sharp dip around $t \sim 1.4$ $(GeV/c)^2$, up to ISR energies. The position of the dip is observed to move toward smaller |t| values, while the height of the secondary maxima grows in the ISR energy range. At much lower energies, no dip is observed in the differential cross-section distribution for proton-proton scattering, but only a break of slope can be observed at $|t| \sim 1.5$ $(GeV/c)^2$.

PRESENT WORK

An effort is made to parameterize the positions of the diffraction dip and the secondary maxima, for proton-proton elastic scattering. From the experimental data, it has been found that the position of the dip is nearly proportional to the total cross-section σ_{tot}. In the present work, a proportionality constant is adjusted to calculate the position of the dip (t_{dip}) as a function c.m. energy, i.e.,
The position of the dip,

$$t_{dip} = X / \sigma_{tot} \quad .....(4)$$

Where, X is a proportionality constant, having a fitted value 57.33.

The fitting of the value of X has been considered for the batter agreement with the experimental data. Similarly, the position of the secondary maxima has been parameterized as,
The position of the secondary maxima,

$$t_{max} = Y / \sigma_{tot} \quad .....(5)$$

Where, Y is another proportionality constant, having a fitted value 78.20. This value of Y is found to be most suitable for the batter agreement with the experimental data.
The differential cross-section at the dip $(d\sigma/dt)_{dip}$ and at the secondary maxima $(d\sigma/dt)_{second\ max}$ have been parameterized as a function of c.m. energy, on the basis of geometrical scattering (Negy, E. *et al.*, 1979). The energy dependence of the differential cross-section at the dip has been parameterized as,

$$(d\sigma/dt)_{dip} = \alpha\ [\exp(\beta\ t_{dip})].(\sigma_{tot})^2 \quad .....(6)$$

Where, α and β are two adjustable parameters. The value of α and β are fitted for fair agreement with the experimental data and are found to be $\alpha = 3.3 \times 10^{-7}$ and β = 1.8.
Similarly, the differential cross-section at the secondary maxima has been parameterized as,

$$(d\sigma/dt)_{second\ max} = \alpha'\ \exp[\beta'\ t_{max}\ (t_{max} - 1.935)].(\sigma_{tot})^2 \quad .....(7)$$

Where, $\alpha' = 4.19 \times 10^{-4}$ and β' = 1.45 are found to be most suitable.

RESULTS AND DISCUSSION

The calculated values of the positions of the dip (t_{dip}) and of the secondary maxima (t_{max}) are presented in the Table-1. And the calculated values of the differential scattering cross-sections at the dip and at the secondary maxima are presented in the Table-2. The calculations have been done at different c.m. energies from 5.00 GeV. to 2000 GeV. The variation of the positions of the dip (t_{dip}) and of the secondary maxima (t_{max}) with c.m. energies are shown in Fig. 1 and the variation of differential scattering cross-sections at the dip $(d\sigma/dt)_{dip}$ and at the secondary maxima $(d\sigma/dt)_{second\ max}$ with c.m. energies are shown in Fig. 2. The position of the dip may be assumed to be the last point of fast decreasing differential cross-section and the position of the secondary maxima may be assumed to be the last point of the increasing differential cross-section.
The most salient feature of the elastic differential cross-section for p-p scattering is the presence of a pronounced peak around the forward direction, which decreases almost exponentially. As energy increases, the slope of p-p forward peak becomes steeper indicating, in optical analogy, an expansion of the interaction radius, proportional to $\sqrt{\sigma_{tot}}$. The results of the present parameterization show the same proportionality. The position of the secondary maxima is also s-dependent. The fitting shows an excellent agreement with the experimental data.

Table1: Positions of the dip (T_{dip}) and of the secondary maxima (T_{max}) in the proton-proton elastic scattering

S.No.	c.m. Energy ($\sqrt{s}$) GeV	Calculated (T_{dip}) $(GeV/c)^2$	Experimental (T_{dip}) $(GeV/c)^2$	Calculated (T_{max}) $(GeV/c)^2$	Experimental (T_{max}) $(GeV/c)^2$
1.	5.00	1.443	---	1.972	---
2.	5.80	1.462	---	1.986	---
3.	7.10	1.480	---	2.021	---
4.	9.80	1.494	1.524 ± 0.008	2.042	2.024 ± 0.006
5.	13.00	1.494	1.465 ± 0.006	2.041	1.983 ± 0.006
6.	18.00	1.475	1.538 ± 0.007	2.014	1.994 ± 0.005
7.	20.00	1.465	---	2.003	---
8.	23.40	1.450	1.440 ± 0.003	1.980	1.971 ± 0.004
9.	26.00	1.437	---	1.960	---
10.	30.50	1.416	1.410 ± 0.003	1.934	1.932 ± 0.003
11.	44.60	1.359	1.370 ± 0.005	1.857	1.918 ± 0.003
12.	52.80	1.332	1.340 ± 0.006	1.820	1.813 ± 0.004
13.	62.10	1.304	1.310 ± 0.012	1.776	1.807 ± 0.004
14.	100.0	1.216	---	1.661	---
15.	200.0	1.087	---	1.486	---
16.	630.0	0.883	---	1.232	---
17.	800.0	0.858	---	1.173	---
18.	1000.0	0.826	---	1.129	---
19.	2000.0	0.736	---	1.005	---

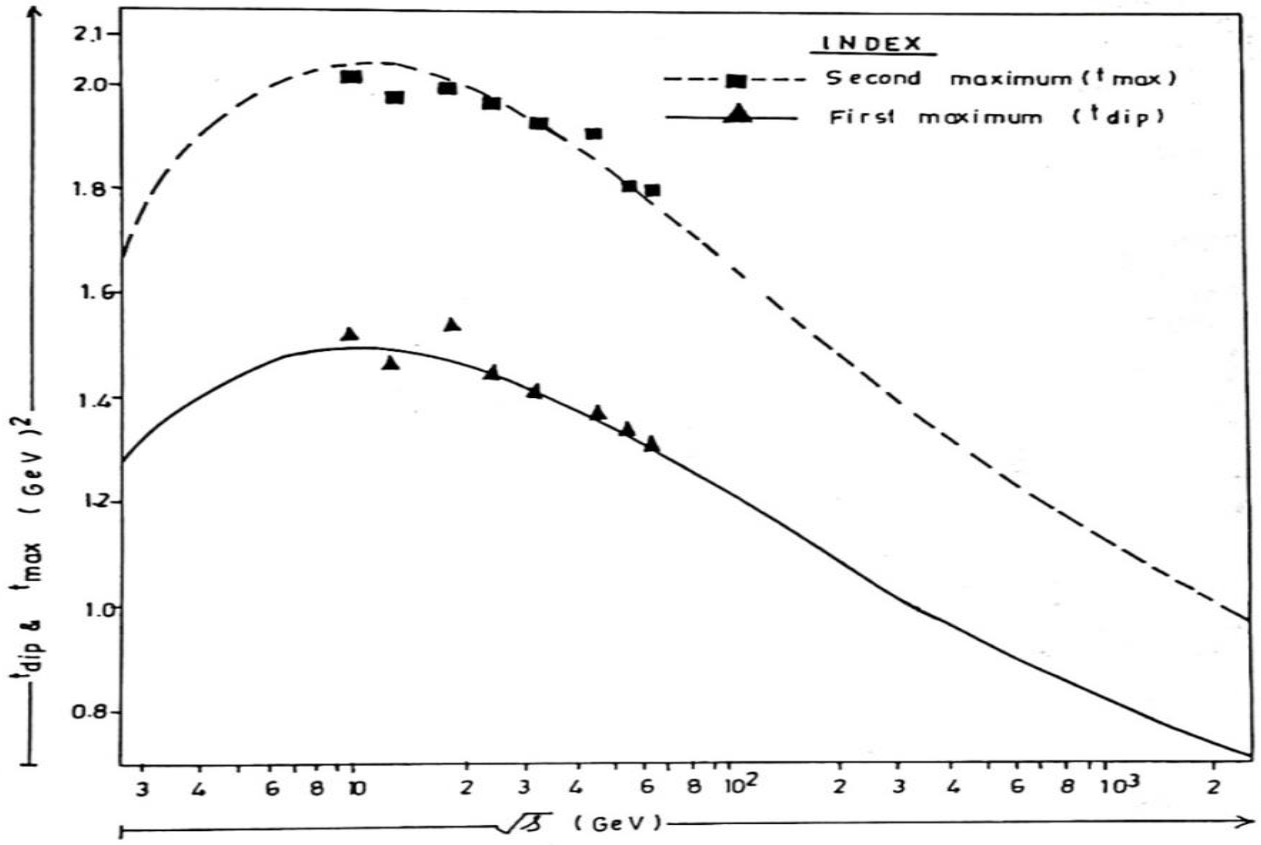

Fig. 1: Positions of the dip (t_{dip}) and of the secondary maxima (t_{max}) at different energies between 3 GeV and 2 TeV. The solid curve represents the position of the dip and the dashed curve represents the position of the secondary maxima

Table 2: Differential scattering cross-sections at the dip $(d\sigma/dt)_{dip}$ and at the Secondary maxima $(d\sigma/dt)_{second\ max}$ for proton-proton scattering

S.No.	c.m. Energy ($\sqrt{s}$) GeV	Calculated $(d\sigma/dt)_{dip}$ (mb)	Experimental $(d\sigma/dt)_{dip}$ (mb)	Calculated $(d\sigma/dt)_{sec.max}$ (mb)	Experimental $(d\sigma/dt)_{sec.max}$ (mb)
1.	5.00	4.400 x 10^{-4}	---	4.65 x 10^{-5}	---
2.	5.80	3.605 x 10^{-4}	---	4.85 x 10^{-5}	---
3.	7.10	2.667 x 10^{-4}	---	5.39 x 10^{-5}	---
4.	9.80	1.478 x 10^{-4}	(1.33± 1.2)x 10^{-4}	5.75 x 10^{-5}	(5.82± 1.75)x 10^{-5}
5.	13.00	7.516 x 10^{-5}	(5.21± 2.8)x 10^{-5}	5.73 x 10^{-5}	(5.95± 1.75)x 10^{-5}
6.	18.00	2.380 x 10^{-5}	(2.08± 1.3) x 10^{-6}	5.28 x 10^{-5}	(5.35± 2.4) x 10^{-5}
7.	20.00	1.430 x 10^{-5}	---	5.10 x 10^{-5}	---
8.	23.40	4.780 x 10^{-6}	(4.0± 0.9) x 10^{-6}	4.77 x 10^{-5}	(4.5± 0.30) x 10^{-5}
9.	26.00	1.370 x 10^{-6}	---	4.50 x 10^{-5}	---
10.	30.50	0.080 x 10^{-6}	(0.5± 0.08) x 10^{-6}	4.20 x 10^{-5}	(4.2± 0.30) x 10^{-5}
11.	44.60	1.071 x 10^{-5}	(13.4± 1.5) x 10^{-6}	5.17 x 10^{-5}	(5.2± 0.30) x10^{-5}
12.	52.80	1.794 x 10^{-5}	(1.98± 0.2) x10^{-5}	5.67 x 10^{-5}	(5.81± 0.3) x 10^{-5}
13.	62.10	2.927 x 10^{-5}	(2.26± 0.4) x 10^{-5}	6.31 x 10^{-5}	(6.31± 0.5) x 10^{-5}
14.	100.0	6.016 x 10^{-5}	---	8.10 x 10^{-5}	---
15.	200.0	1.011 x 10^{-4}	---	1.10 x 10^{-4}	---
16.	630.0	1.455 x 10^{-4}	---	1.47 x 10^{-4}	---
17.	800.0	1.547 x 10^{-4}	---	1.53 x 10^{-4}	---
18.	1000.0	1.618 x 10^{-4}	---	1.57 x 10^{-4}	---
19.	2000.0	1.755 x 10^{-4}	---	1.63 x 10^{-5}	---

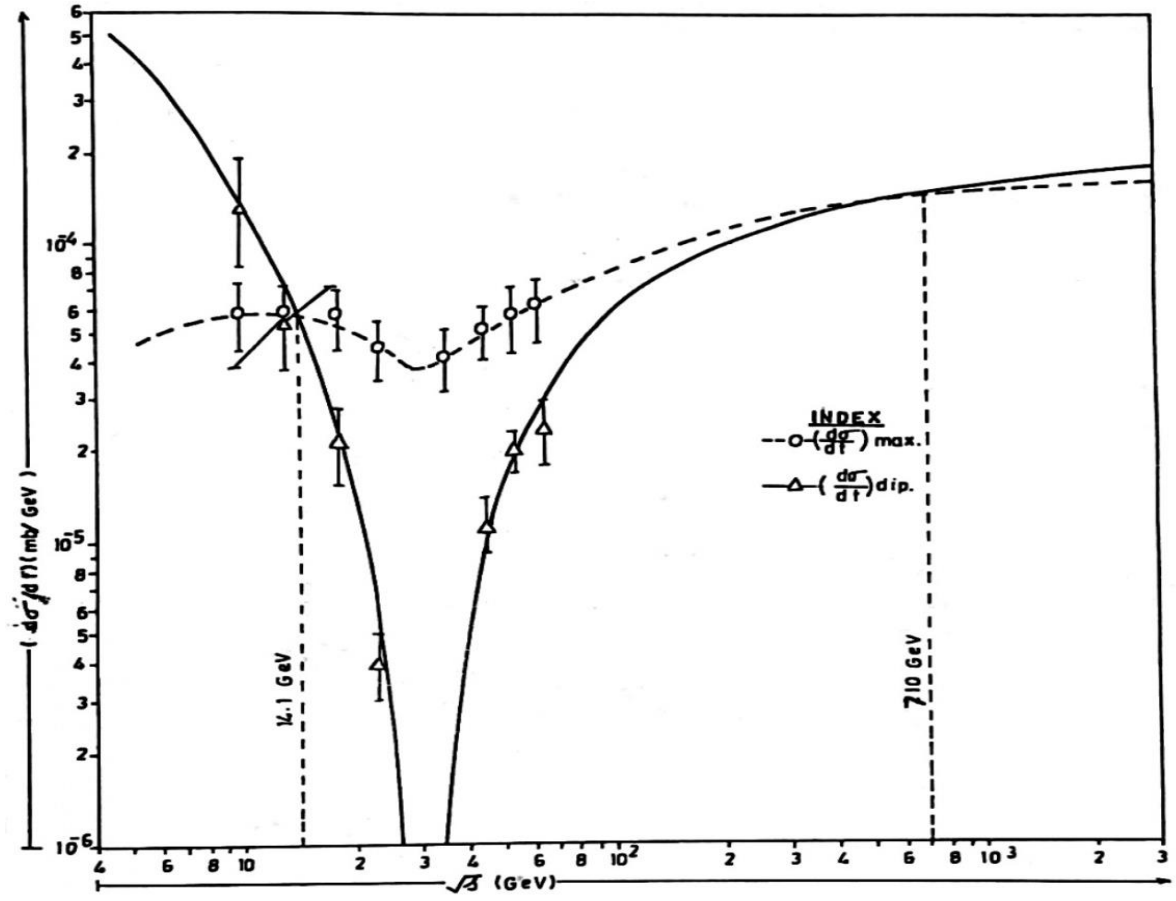

Fig. 2: Energy dependence of Differential scattering cross-sections at the dip $(d\sigma/dt)_{dip}$ and at the secondary maxima $(d\sigma/dt)_{second\ max}$. The solid curve represents $(d\sigma/dt)_{dip}$ and the dotted curve shows $(d\sigma/dt)_{second\ max}$ at different energies.

The differential cross-section at the dip $(d\sigma/dt)_{dip}$ is observed to decrease on increasing c.m. energy up to 30 GeV and to increase again. Also the differential cross-section at the secondary maxima $(d\sigma/dt)_{second\ max}$ decreases on increasing c.m. energy ($\sqrt{s}$) towards 30 GeV, but it shows a decreasing character below 10.5 GeV also. For high energies ($\sqrt{s}$ > 30 GeV), the $(d\sigma/dt)_{dip}$ and $(d\sigma/dt)_{second\ max}$ both increase with c.m. energies, but the rate of increase of $(d\sigma/dt)_{dip}$ is lower than that of $(d\sigma/dt)_{second\ max}$.

In a diffractive picture, the imaginary part is assumed to be the dominant scaling component of the scattering amplitude and is supposed to vanish at the position of the dip, where only a small real part contributes to the cross-section. This interpretation is supported by the fact that the ratio ρ of the real to imaginary part of the scattering amplitude, goes through zero at about the energy at which the dip is sharpest. In the similar manner, it is assumed in the present work, that the differential cross-section at secondary maxima should depend on the position of the secondary maxima and its deviation from the position of the maximum height of the secondary maxima.

CONCLUSION

The positions of the dip (t_{dip}) and of the secondary maxima (t_{max}) shift inward, generally, on increasing the incident energies. The differential scattering cross-section at the dip $(d\sigma/dt)_{dip}$ depends not only on the behavior of $(\sigma_{tot})^2$, but it depends also on the t-dependent behavior of the differential cross-section $(d\sigma/dt)$ in the peak region. The differential cross-section at the secondary maxima $(d\sigma/dt)_{second\ max}$ depends on the position of the secondary maxima and also on the deviation of its position from the position of the secondary maxima of maximum height.

REFERENCES

1. Abazov, V.M. *et al.*, (2012): Observation of a narrow mass state decaying in p-$\bar{p}$ collisions at 1.96 TeV. Phys. Rev. D 86; 12009.
2. Alsad, Z. *et al.*, (1983): Proton-proton elastic scattering at 50 GeV/c incident momentum, Phys. Lett. B 128 (1983); 124.
3. Amaldi, U. *et al.*, (1973): Energy dependence of pp total cross-section for c.m. energies 23-25 GeV., Phys. Lett. B 44; 112.
4. Amaldi, U. *et al.*, (1977): Real part of the forward pp scattering amplitude, Phys. Lett. B 66; 390.
5. Amos, N.A. *et al.*, (1990): A Luminosity independent measurement of pp total cross-section, Phys. Lett. B 243; 158.
6. Avila, C. *et al.*, (2002): The ratio of the real to imaginary part of p-$\bar{p}$ forward elastic scattering amplitude, Phys. Lett. B 537; 41.
7. Breakstone, A. *et al.*, (1984): A measurement of pp and p-$\bar{p}$ elastic scattering at ISR energies, Nucl. Phys. B 248; 253.
8. Bronzan, J.B. *et al.*, (1974): Obtaining real parts of scattering amplitudes directly from cross-section data, Phys. Lett. B 49; 272.
9. Burg, J.P. *et al.*, (1982): Experimental results on pp forward elastic scattering, Phys. Lett. B 109; 124.
10. Castaldi, R. *et al.*, (1985): Elastic scattering ana total cross-sections at very high energies, Ann. Rev. Nucl. Part. Sci. 35; 351.
11. Gauron, P. and Nicobscus, B. (1998): Similarities and Differences Between pp and p-$\bar{p}$ scattering at TeV energies and Beyond., Nucl. Phys. B 299; 640.
12. Giacomelli G. and M. Jacob, (1979): Physics at CERN-ISR, Phys. Rep. 55; 1.
13. Kaspar, J. *et al.*, (2011): Phenomenological models of elastic nucleon scattering and predictions for LHC, Nucl. Phys. B 843; 84.
14. M.M. *et al.*, (2016): Slope, curvature and higher parameters in pp and p-$\bar{p}$ scattering, Phys. Rev. D 93; 114009.
15. Negy, E. *et al.*, (1979): Measurement of elastic scattering at large momentum transfer, Nucl. Phys. B 150; 221.